Photoinduced Transient Absorbance Spectra of P840/P840$^+$ and the FMO Protein in Reaction Centers of *Chlorobium vibrioforme*

Ilya R. Vassiliev,* Bodil Kjær,† Gregory L. Schorner,* Henrik V. Scheller,† and John H. Golbeck*
*Department of Biochemistry and Molecular Biology, The Pennsylvania State University, University Park, Pennsylvania 16802 USA; and †Department of Plant Biology, The Royal Veterinary and Agricultural University, DK-1871 Frederiksberg C, Denmark

ABSTRACT The kinetics of photoinduced absorbance changes in the 400-ns to 100-ms time range were studied between 770 and 1025 nm in reaction center core (RCC) complexes isolated from the green sulfur bacterium *Chlorobium vibrioforme*. A global, multiple stretched-exponential analysis shows the presence of two distinct but strongly overlapping spectra. The spectrum of the 70-μs component consists of a broad bleaching with two minima at 810 and 825 nm and a broad positive band at wavelengths greater than 865 nm and is assigned to the decay of ^{3}Bchl *a* of the Fenna-Matthews-Olson (FMO) protein. The contribution of the 70-μs component correlates with the amount of FMO protein in the isolated RCC complex. The spectrum of the 1.6-μs component has a sharp bleaching at 835 nm, a maximum at 805 nm, a broad positive band at wavelengths higher than 865 nm, and a broad negative band at wavelengths higher than 960 nm. When the RCC is incubated with inorganic iron and sulfur, the 1.6-μs component is replaced by a component with a lifetime of $\sim$40 μs, consistent with the reconstruction of the F_X cluster. We propose that the 1.6-μs component results from charge recombination between P840$^+$ and an intermediate electron acceptor operating between A_0 and F_X. Our studies in *Chlorobium* RCCs show that approaches that employ a single wavelength in the measurement of absorption changes have inherent limitations and that a global kinetic analysis at multiple wavelengths in the near-infrared is required to reliably separate absorption changes due to P840/P840$^+$ from the decay of ^{3}Bchl *a* in the FMO protein.

INTRODUCTION

The photosynthetic apparatus of green sulfur bacteria consists of three main elements, the reaction center (RC), Fenna-Matthews-Olson (FMO) Bchl *a*-protein, and the chlorosome (Olson, 1998), and represents one of the most extensive systems for light energy conversion known among phototrophic organisms. The chlorosomes are composed mostly of self-aggregated bacteriochlorophyll (Bchl) *c*, Bchl *d*, or Bchl *e*, hundreds of quinones, some waxes and carotenoids, and relatively small amounts of protein (Olson, 1998). The exact function of the 41-kDa Bchl *a*-containing FMO protein is not resolved, and although it has been suggested that FMO can participate in energy transfer from the chlorosome to the RC (Schmidt and Trissl, 1998; Zhou et al., 1994), other data indicate that the energy absorbed by FMO is not coupled to the RC (Kramer et al., 1996; Neerken et al., 1998). The RC complex consists of five subunits: a homodimer of the 65-kDa photochemically active PscA protein, the 32-kDa 2[4Fe-4S] PscB protein, the 24-kDa cytochrome c_{551} of the PscC protein, a polar 17-kDa PscD protein of unknown function, and the FMO protein (for a review see Feiler and Hauska, 1996). A minimum RC core (RCC) complex composed of only the PscA and PscB polypeptides has been isolated by Amesz and co-workers (Francke et al., 1997). The protein composition and the stoichiometry of cofactors in the analogous RC of oxygenic photosynthesis, photosystem (PS) I, are strikingly similar for different species of cyanobacteria isolated using different chemical procedures (Golbeck 1994). In contrast, the relative protein content (especially of PscC and FMO) and the activity of the electron transfer cofactors vary significantly in RC complexes from different species of green sulfur bacteria using different biochemical procedures.

The primary electron donor, P840 (a Bchl *a* dimer), was first identified in whole cells of *Chloropseudomonas ethylicum* (actually a mixed culture containing *Prosthecochloris aestuarii* and *Desulfuromonas acetoxidans*) by a photobleaching at 840 nm (Sybesma and Vredenberg, 1963). Major bleaching at 830 and 842 nm and a minor bleaching at 790 nm were observed later in light-induced and chemically oxidized-minus-reduced difference spectra of RC complexes isolated from *Chlorobium ethylicum* (Fowler et al., 1971) and *Chlorobium limicola* f. *thiosulfatophilum* (Olson et al., 1973). The photoinduced difference spectrum of P840$^+$/P840 was measured at wavelengths up to 1250 nm, and a positive absorbance change at 1157 nm was ascribed to the oxidation of P840 (Olson et al., 1976). P840$^+$ is reduced within tens of microseconds from the secondary donor, cytochrome c_{551} (Albouy et al., 1997, Oh-Oka et al., 1997), whereas the primary acceptor A_0, a Chl-*a*-like pigment (Van de Meent et al. 1992), is reduced within 30 ps (Kramer et al, 1996; Schmidt and Trissl, 1998). The presence of a quinone-type secondary acceptor (A_1) in the *Chlorobium* RC complex is still a matter of controversy (Kjær et al., 1998; Kusumoto et al., 1999). RC complexes of green sulfur bacteria contain three [4Fe-4S] clusters that apparently comprise a sequence of terminal electron cofac-

Received for publication 18 July 2000 and in final form 2 March 2001.

Address reprint requests to Dr. John H. Golbeck, Department of Biochemistry and Molecular Biology, The Pennsylvania State University, S.310 Frear Hall, University Park, PA 16802. Tel.: 814-865-1162; Fax: 814-863-7024; E-mail: jhg5@psu.edu.

0006-3495/01/07/382/12 $2.00

tors similar to that of F_X, F_B, and F_A of PS I (Hager-Braun et al., 1997; Scott et al., 1997; Vassiliev et al., 2000). The rates of forward electron transfer between the iron-sulfur clusters as well as the rates of their back-reactions with $P840^+$ are largely a matter of conjecture.

A number of kinetic studies of P840 were made using transient absorbance spectroscopy at wavelengths around 835–840 nm (Miller et al., 1992; Okkels et al., 1992; Francke et al., 1997; Neerken et al., 1998; Schmidt et al., 2000), where a bleaching of Bchl occurs. Transient absorbance spectra of RC preparations from different green sulfur bacteria have been measured in the near-infrared (NIR) at wavelengths up to 900 nm (Kramer et al., 1996; Oh-Oka et al., 1995a,b). The transient absorbance spectrum of membrane fragments of *Prosthecochloris aestuarii* was measured between 760 and 880 nm and was found to consist of a 25-μs component ascribed to the reduction of $P840^+$ from cyt c_{551} and a 165-μs component that represents the decay of the RC triplet (Franken and Amesz, 1997).

Although the electron transfer reactions in RCs of green sulfur bacteria have been extensively studied during the last decade, the time constants of these reactions as well as the presence of an intermediate acceptor analogous to A_1 of PS I are still a matter of debate. Because biochemical removal (albeit incomplete) of the FMO protein inevitably leads to the degradation of the [4Fe-4S] clusters, the most photoactive preparations of RCs necessarily contain substantial amounts of other pigments that interfere with P840 absorbance changes. Consequently, approaches that utilize measurements of redox changes at a single wavelength have an inherent limitation.

Because wavelengths around 840 nm can, in principle, induce oxidation of P840, the use of probe wavelengths at lower energy, i.e., farther in the infrared region of the spectrum, should be useful for studies of P840 photochemical reactions. Knowledge of this part of the transient absorbance spectrum of P840 would be a particular advantage in intact cells or isolated chlorosome-containing membranes where even a low ambient light leads to reduction of P840. On the one hand, a combination of monochromators with conventional sources may not provide enough light to allow kinetic measurements on the nanosecond to microsecond time scales with a sufficiently high signal-to-noise (S/N) ratio. On the other hand, tunable lasers may not have sufficient output stability required for accurate measurements on these and longer time scales.

Here, we describe the experimental setup of a tunable laser spectrophotometer that, in combination with a global analysis of absorbance changes in the NIR, overcomes these limitations. The aim of this work is to resolve the spectra of different kinetic components in the NIR in RCC complexes of *Chlorobium vibrioforme*. Our studies show that *Chlorobium* RCCs require a global kinetic analysis at several wavelengths in the NIR to reliably resolve absorption changes due to redox changes in $P840/P840^+$. Such analysis shows the occurrence of two overlapping spectra, one attributed to $P840^+$ reduction (~1.6-μs lifetime) and the other to the decay of ^{3}Bchl *a* in the FMO protein (~40–70-μs lifetime). The substitution of the 1.6-μs component by a component with a lifetime of ~40 μs following incubation with inorganic iron and sulfur implies that the 1.6-μs component represents the recombination of an intermediate electron acceptor with $P840^+$.

MATERIALS AND METHODS

Isolation of the RCC complexes

Chlorobium vibrioforme strain NCIB 8327 was grown as previously described (Okkels et al., 1992), and the RCCs were prepared using *n*-dodecyl-β-D-maltoside (β-DM) to solubilize the membranes under strict anaerobic conditions (Kjær et al., 1994). The final step in the isolation utilized gel-filtration chromatography, and several fractions from the column were collected. In this work, two types of samples were studied: an early eluting fraction (fraction 1) and a late eluting fraction (fraction 2), which differed in their FMO content. The sample stocks (BChl *a* concentration, 100 μM) were stored in airtight glass vials at −80°C.

Iron-sulfur clusters were inserted into the RCCs in a manner similar to that described previously (Parrett et al. 1990) but under anaerobic conditions. To 400 μl of 5 mg/ml RCC solution, 16 μl of β-mercaptoethanol, 6.0 μl of a 60 mM $FeCl_3$ solution, and 6.0 μl of a freshly prepared 60 mM Na_2S solution were added. All additions were performed drop-wise at 20-min intervals. The reconstitution mixture was allowed to incubate in an airtight vial overnight at 279 K. The vial was transferred to an anaerobic chamber, and the excess iron and sulfide were removed by repeated dilution with 50 mM Tris-HCl, pH 8.3, followed by concentration in a YM-100 Microcon concentrator (Millipore Corp., Bedford, MA). A control sample was prepared in the same manner, except that the $FeCl_3$ and Na_2S were not added.

Electrophoresis was carried out in 8–25% gradient gels prepared according to Fling and Gregerson (1986). The gel was stained with Coomassie brilliant blue. For optical measurements the samples were suspended in 50 mM Tris buffer (pH 8) with 0.05% β-DM at Bchl *a* concentrations from 10 or 20 μM (as indicated in the figure legends). Unless otherwise indicated, 50 μM *N*,*N*,*N*′,*N*′-tetramethylphenylenedyamine (TMPD) and 10 mM sodium ascorbate were used as the electron donors to $P840^+$ to ensure its complete reduction between flashes. All chemicals were added to the sample inside an anaerobic chamber using anaerobic solutions.

Measurement of chemically induced differential spectrum of $P840^+/P840$

Chemically induced difference spectra were recorded on a Beckman DU-60 spectrophotometer interfaced to a personal computer. The spectrum of the oxidized sample was measured after addition of 5 mM potassium ferricyanide to the sample (BChl *a* concentration, 10 μM) in 50 mM Tris buffer (pH 8) containing 0.05% β-DM. The spectrum of the reduced sample was measured following addition of 50 μM TMPD and 10 mM sodium ascorbate. The difference between these two spectra is reported.

Transient absorbance spectroscopy

Transient absorbance changes in the NIR were measured with a laboratory-built double-beam spectrophotometer. The sample was placed in a 10-mm × 4-mm quartz cuvette with an airtight stopper. The excitation beam was provided by a frequency-doubled (λ = 532 nm), Q-switched Nd:YVO_4 laser (DCR-11, Spectra Physics, Mountain View, CA) and was

expanded to a 15-mm-diameter spot and oriented normal to the longer side of the cuvette. The pulse width at half-maximum was 10 ns, and the flash energy was attenuated by varying the Q-switch delay and using a combination of neutral density filters. In all experiments (except for that presented in Fig. 4) the energy of the excitation flash was ~80 mJ. The measuring beam, which was oriented normal to the shorter side of the cuvette, was provided by a titanium-sapphire laser (model TI-SPB, Schwartz Electro-Optics, Orlando, FL) pumped with a diode-pumped, frequency-doubled CW Nd:YVO_4 (model Millenia, Spectra Physics) at 5.4-W output power. Wavelengths from 770 to 905 nm, with maximum output of 200 mW at 850 nm, were provided by the mid-band set of mirrors of the titanium-sapphire laser. Wavelengths from 900 to 1025 nm were provided by the long-band set of mirrors, but the beam stability was poorer and the output power was lower (~50 mW at 960 nm). The measuring beam was split by a nonpolarizing broadband beam splitter (~1:1 ratio); the signal beam was attenuated with neutral density filters to maintain a non-actinic intensity and passed through the cuvette, while the reference beam was passed through a variable-density filter wheel alongside the cuvette to equalize the intensities of both beams. Both beams were directed toward a pair of reverse-biased silicon photodiodes (United Detector Technology, Hawthorne, CA; model PIN-10D) shielded by RG-10 cutoff filters. The photocurrents were converted into voltages with 100-Ω resistors, and the difference between the signal and reference was taken in real time at 8-bit vertical resolution using a Tektronix 11A33 DC-coupled differential comparator (150-MHz bandwidth) plugged into a Tektronix DSA 601 digital signal analyzer (Tektronix, Beaverton, OR).

Kinetics were acquired simultaneously on two different time scales (4096 points at 100 μs/point in the main window and 5120 points at 100 ns/point in the zoom window). The sweep was triggered by a PD 40 avalanche photodiode (Opto-Electronics, London, Ontario, Canada), which monitored stray light of the excitation laser pulse via a Tektronix 11A52 amplifier (600-MHz bandwidth). The DSA 601 was interfaced to a Power Macintosh computer via a NB-GPIB/TNT (National Instruments, Austin, TX) board. The protocol for transfer of each pair of kinetics and their storage as separate binary files on the computer hard drive was implemented in a LabView v. 4.1 (National Instruments) virtual instrument (VI) integrating Tektronix DSA 601.VI (from National Instruments) and LabView to Igor Binary.VI (written by G. W. Johnson, Lawrence Livermore National Laboratory, Livermore, CA). After completion of each measurement the data files were processed by a program written in Igor Pro v. 3.14 (Wavemetrics, Lake Oswego, OR) to average the data and to discard the traces containing vibration-related and electrical artifacts. The non-overlapping kinetics corresponding to different time domains were linked to generate the overall trace. The data were reduced as necessary by point averaging using a variable-widths window, the widths increasing as an exponential function of time. The absorbance change was calculated according to the formula, $\Delta A = -0.434\ln(1 + \Delta I/I)$. Depending on the quality of the signal, 10 to 50 kinetic scans were averaged at each wavelength, normally at 5-nm intervals. Due to lower S/N ratio at long wavelengths, and given a broader and unstructured spectrum in this region, the kinetics were taken at greater wavelength intervals to allow more averages at a given wavelength per unit time.

Kinetic analysis was performed using a nonlinear regression Marquardt algorithm in Igor Pro v. 3.14 on a 300-MHz G3 Macintosh computer. Because pure multi-exponential fits appeared to give poor results, an Igor program was written to implement the fit to n stretched exponentials: $A(t) = \Sigma_{i=1}^{n} A_i \exp(-(t/\tau_i)^{\beta_i}) + B$, where $A(t)$ is the amplitude of absorbance change at a time t, A_i is the amplitude of individual component, τ_i is its lifetime, and β_i is a dimensionless parameter ($0 < \beta_i \leq 1$). If β of a particular term converges to 1, then this term becomes a pure exponential. B is the amplitude of the baseline offset, which accounts for slow components with lifetimes that cannot be determined on the applied acquisition time scale. The quality of the fit was evaluated by analysis of χ^2, standard errors of the parameters, and the residuals of the fit. The results of data analyses at individual wavelengths were then used for fitting the whole set of data to global lifetimes and global stretch parameters using the Global Fit procedure included in the Igor Pro v. 3.14 distribution package, with minor modification of the procedure source code for storage and presentation of results.

RESULTS

Comparison of preparations differing in FMO content

During the isolation of the RC complex several fractions were collected from the column, and the two most abundant fractions were analyzed by gel electrophoresis. The amount of FMO present in the two preparations was estimated by densitometric scanning of the Coomassie-stained gel. The earlier fraction, referenced as fraction 1, had a higher amount of FMO protein relative to PscA than a later fraction, referenced as fraction 2 (Fig. 1). Assuming that the FMO protein and PscA bind the same amount of dye per milligram of protein, a content of 5.0 and 2.8 copies of the FMO protein per P840 could be calculated in the two fractions. It is also apparent from these gels that the samples are mostly devoid of PscB protein lost during the isolation procedures, and therefore we refer to them as the reaction center core (RCC) complexes. The loss of the PscB subunit is consistent with EPR data indicating no resonances of F_A and F_B at liquid helium temperatures (not shown). The RCC complexes from these two fractions were then compared by transient absorbance spectroscopy.

Analysis of decay kinetics at selected wavelengths

We first studied the kinetics of flash-induced absorbance changes at 835-, 800-, and 900-nm, wavelengths where the most distinct negative or positive absorbance changes oc-

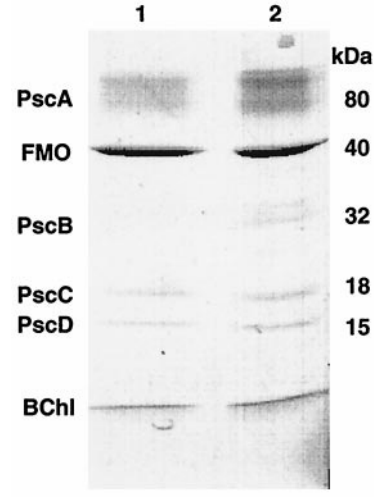

FIGURE 1 SDS-polyacrylamide gel electrophoresis of the RCC samples of FMO-enriched fraction 1 (*left lane*) and fraction 2 (*right lane*).

cur. Fig. 2 shows the kinetics of absorbance changes measured in fraction 1 (left column, *a* and *b*) and fraction 2 (right column, *d--f*). The measuring beam intensity was attenuated at wavelengths below 860 nm to 10–50 mW to ensure lack of an actinic light effect that could result in a decrease in the amplitude of the absorbance change. The maximum amplitude of the absorbance changes occurred in the 825–840-nm region. As seen in the residuals plots in Fig. 2 *c*, at these wavelengths the decay kinetics could not be accurately fit using as many as four to five exponentials with lifetimes ranging from 300 ns to 200 ms, indicating a deviation from pure multi-exponential behavior. This deviation may result from a distribution of rates of photochemical processes that occur in a mixture of RCC complexes. Because the seemingly acceptable solution required as many as six exponentials, we attempted to minimize the number of components necessary for the fit by applying a multiple stretched-exponential equation. Such an equation (see Materials and Methods) provides a robust solution for kinetics with distributed rates; it has been applied to studies of the dielectric relaxation in the solid state (Montrol and Bendler, 1984), and it has been successfully used to fit absorbance changes in RC complexes of green filamentous bacteria at low temperatures (Becker et al., 1991). In our analysis, we sought to obtain the best fit of the kinetics by employing a minimum number of stretched exponential components and to obtain a symmetrical pattern of the residuals plot at a minimized χ^2. The solution employing three stretched exponentials had a slightly higher χ^2 than for six exponentials (Fig. 2 *c*), but addition of another stretched exponential (or pure exponential) component led to high standard errors of the parameters. Such an analysis of traces with the highest S/N ratio at different wavelengths gave similar values of lifetimes (τ) and stretch parameters (β) for three distinct kinetic components. The lifetime of the fastest component ranged from 1 to 2 μs, with the stretch parameter ranging from 0.3 to 0.75. The intermediate component had a lifetime of 30–100 μs with a stretch parameter of 0.6–1. The parameters of the slowest component were cleanly resolved only at wavelengths distant from the edges of the laser tuning ranges. The lifetime of this component varied from 8 to 100 ms (with $\beta = 0.6$–1), with a positive absorbance change at all wavelengths. Its amplitude was 1–2% relative to the sum of absolute amplitudes of the two fastest components at 830–840 nm. Due to low power and poor stability of the measuring beam on the milliseconds time scale at wavelengths higher than 920 nm, this component could not be reliably fitted. A baseline was assumed in addition to two faster components by restricting the fitting time range to 1 ms.

We compared the kinetics of two fractions of RCCs at different wavelengths, 835 nm and 800 nm. At the latter wavelength the kinetics consists predominantly of the 65-μs component (see Fig. 2, *b* and *e*). Comparison of Fig. 2, *a* and *b* (fraction 1), with Fig. 2, *d* and *e* (fraction 2) shows that 1) at 835 nm the ratio of the slower (31–63-μs) component to the faster component (1.6–1.8 μs) is considerably higher in the FMO-enriched fraction 1 and that 2) the amplitude of the absorbance change at 800 nm relative to that at 835 nm is higher in the FMO-enriched fraction 1 than in fraction 2. This further indicates that there are two components of different origin with absorbance changes in the NIR.

Global analysis

Following the analysis of the individual kinetics at all studied wavelengths, the resulting lifetimes and stretch parameters were averaged to be used, along with the amplitudes derived for each wavelength, as initial assumptions for the global multiple stretched-exponential fit. This analysis was performed only for the RCC-enriched fraction (fraction 2). Because of the poor resolution of the slowest component at wavelengths above 860 nm, a global fit to three stretched exponentials was performed at wavelengths to 860 nm, whereas at higher wavelengths the kinetics were fitted in the 400-ns to 1-ms time domain to two stretched exponentials and a baseline. The global analyses in these two spectral regions gave similar results: the fast component had $\tau = 1.6$ μs and $\beta = 0.31$ in the first spectral range, and $\tau = 1.6$ μs with $\beta = 0.5$ in the second spectral range. The intermediate component had $\tau = 70$ μs and $\beta = 0.99$ in the first spectral range, and a $\tau = 107$ μs and $\beta = 0.61$ in the second spectral range. The spectra of the amplitudes of the 1.6-μs and 70–107-μs components are shown in Fig. 3 *a*, along with the overall fit curves at several representative wavelengths (Fig. 3, *b* and *c*). Consistent with the results of the free running fit, the amplitude of the slowest component varied from 0.1×10^{-3} to 0.6×10^{-3} OD units in the whole range of wavelengths without any apparent spectral features (not shown). As shown in Fig. 3 *a*, the amplitudes of the two resolved kinetic components follow different spectra. The spectrum of the 1.6-μs component is similar in shape to the chemically reduced-minus-oxidized difference spectrum obtained on the same preparation (shown in the bottom of Fig. 3 *a*), whereas the spectrum of the 70-μs component matches closely the spectrum of the ^{3}Bchl *a* decay of FMO protein (see Discussion). Both spectra display a positive change of absorbance at wavelengths between 900 and 950 nm. The reliability of the fit near the crossover region for both components (880–900 nm) was lower due to poor S/N ratio of low-intensity signals that comprise one or more components of a different sign. This is partly a result of the lower stability of the measuring beam at the border of the midband set of Ti-sapphire laser mirrors. At wavelengths above 950 nm, the fast component (1.6 μs) has changed its sign, whereas the slower components have retained their positive sign. Fig. 3, *b* and *c*, shows the kinetics at selected wavelengths with corresponding fit curves.

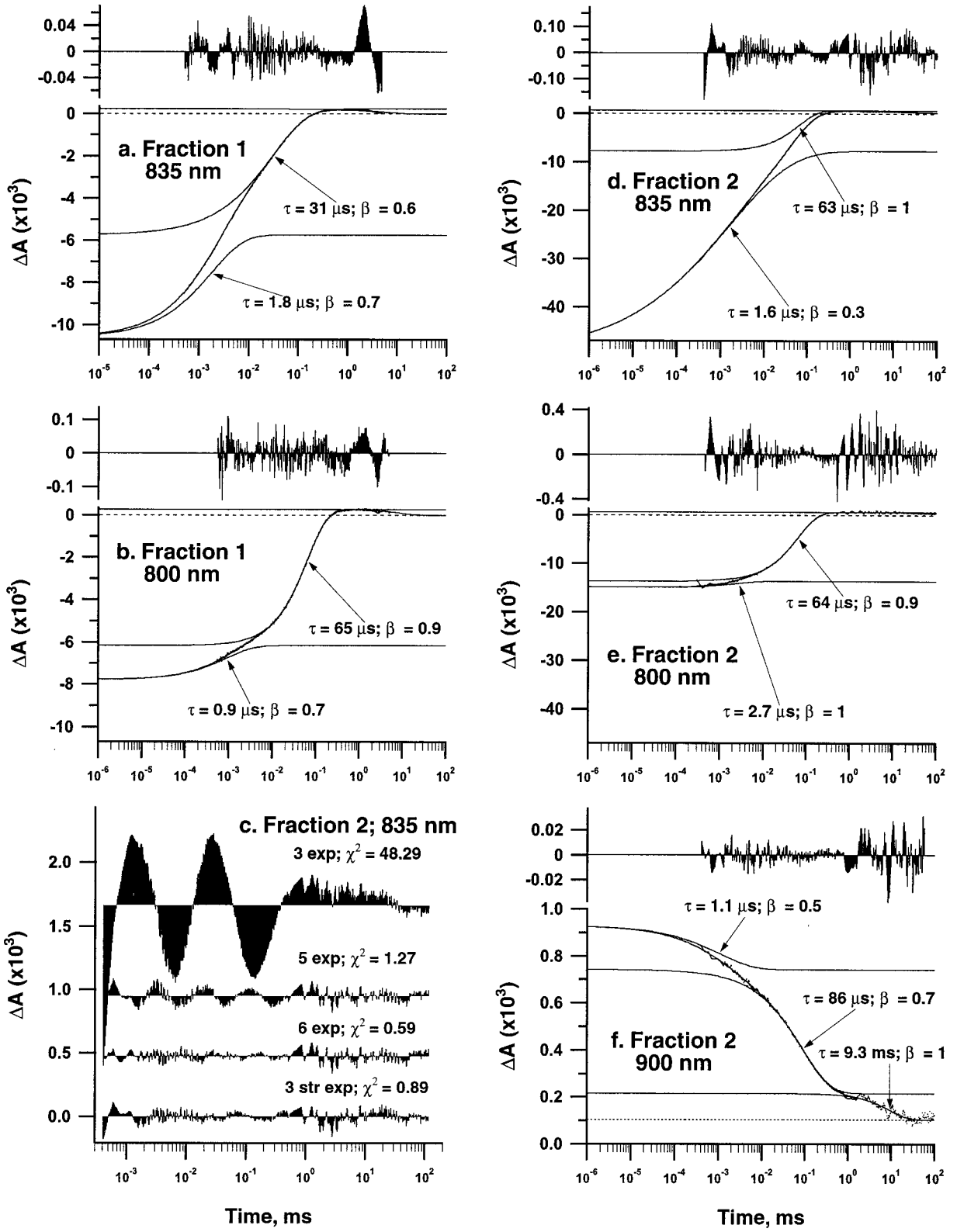

FIGURE 2 Kinetics of absorbance changes measured at different wavelengths in FMO-enriched fraction 1 (*a* and *b*) and in fraction 2 (*d–f*) of RCC complexes isolated from *C. vibrioforme*. Reaction medium (anaerobic) included 50 mM Tris buffer (pH 8), 0.05% β-DM, 50 μM TMPD, and 10 mM Na ascorbate. Bchl *a* concentration was 20 μM (fraction 2) or 10 μM (fraction 1). Each individual component of the multiple stretched-exponential fit is plotted with a vertical offset relative to the next component (with a longer lifetime) or the baseline, the offset being equal to the amplitude of the latter component. Flash energy, 80 mJ; intervals between the flashes, 8 s.

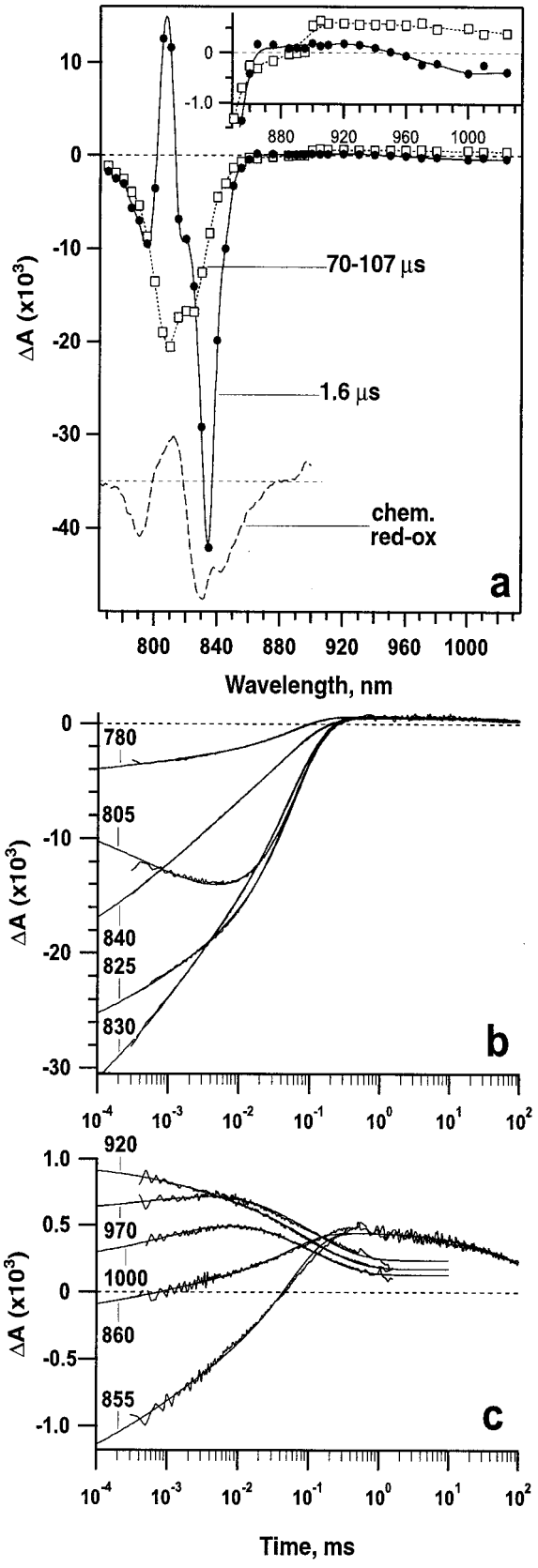

FIGURE 3 (*a*) Spectra of kinetic components of absorbance change in isolated *C. vibrioforme* RCC complexes (fraction 2) derived by global multiple stretched-exponential fit. A chemically induced reduced-minus-oxidized spectrum of the RCC is plotted as a dashed line (with vertical offset relative to the time-resolved spectrum). (*b* and *c*) Kinetics at selective wavelengths and fit curves derived by global analysis. Bchl *a* concentration was 20 μM (10 μM for chemically induced spectrum). Other experimental conditions were as in Fig. 2.

Flash saturation dependence

We next studied the dependence of the kinetics on the energy of the excitation flashes. The kinetics measured at 835 and 800 nm were analyzed by global fitting to the sum of stretched exponentials and a baseline, as described above. As shown in Fig. 4, the flash saturation dependencies of the amplitudes of two components with lifetimes of 1.6 μs and 40 μs in fraction 1 were similar. The flash saturation dependency of the slower component measured at 800 nm was almost identical to that measured at 835 nm (not shown).

Effects of a chemical oxidant

Because the flash saturation dependencies of the 1.6-μs and 40-μs components were nearly identical, we attempted to selectively inhibit the fastest component by adding an oxidant, potassium ferricyanide. In PS I, ferricyanide completely oxidizes P700, and excitation with sufficiently high-energy flashes can induce the generation of ^{3}Chl *a* with its subsequent decay on the tens-of-microseconds time scale (Vassiliev et al., 1997). In the *Chlorobium* RCC complex, however, addition of ferricyanide up to 80 mM results in the near-complete elimination of the slower component and in a considerable suppression of the fast component, its lifetime now being approximated as 730 ns (β = 0.4) (Fig. 5 *a*). Addition of excess reductant (sodium ascorbate and TMPD) lead to the recovery of both components (Fig. 5 *b*), although the recovered amplitudes are lower than without pretreatment by ferricyanide (Fig. 2 *a*). The sensitivity of the 40-μs component to oxidation by ferricyanide agrees with the assessment that this protein contains redox-active regulatory components (Zhou et al., 1994).

Reconstruction of the F_X iron-sulfur cluster

The above results show the presence of two essential kinetic components in the NIR absorbance changes that differ in their spectral signatures. Although the tens-of-microseconds component can be assigned to the decay of the ^{3}Bchl *a* in FMO, and the 1.6-μs component to $P840^+$ reduction, the acceptor in the charge recombination reaction still needs to be identified. Due to apparent loss of PscB revealed by the gel electrophoresis and due to lack of F_A/F_B EPR signals (not shown), the acceptor must be either F_X or an intermediate acceptor between F_X and A_0. In the latter instance, F_X may be lost in the course of the isolation procedure. Hence, it should be possible to re-

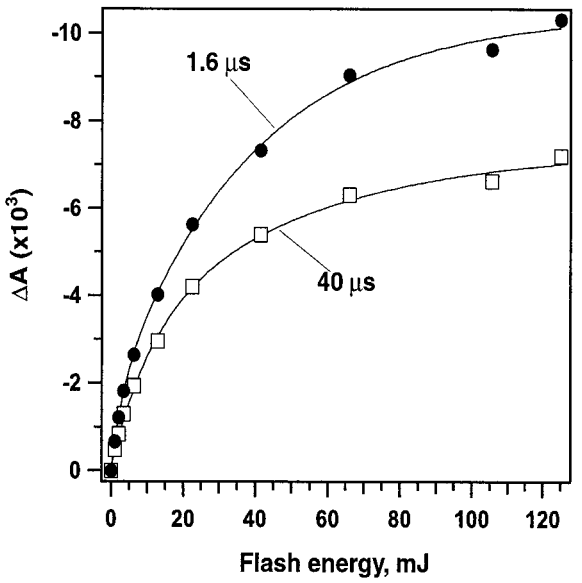

FIGURE 4 Excitation flash energy dependency of two kinetic components' amplitudes (derived from global stretched-exponential analysis of absorbance change at 835 nm) in the *C. vibrioforme* RCC complex (fraction 1). Bchl *a* concentration was 10 μM. Other experimental conditions were as in Fig. 2.

insert the F_X cluster into the $(PsaA)_2$ dimer using inorganic iron and sulfur as demonstrated for F_X in PS I (Parrett et al., 1990). As shown in Fig. 6, both the 835-nm and 910-nm absorbance change were similarly affected when the sample was incubated with $FeCl_3$ and Na_2S. By measuring the absorbance change at 835 nm, we noticed a replacement of the fast, 3.6-μs component with a slower, 22.6-μs component. Even though the lifetimes of the two components revealed upon fitting of the kinetics in the RCCs incubated with $FeCl_3$ and Na_2S were relatively similar (22.6 μs and 44 μs), this two-component solution provided a better fit than using a single stretched exponential. Likewise, a 1.7-μs component was no longer observed at 910 nm after the sample incubation with $FeCl_3$ and Na_2S, but in this case the fit converged to a single 38-μs component and a slower phase fitted with a baseline. Taken together, these results document a replacement of the fast (several microseconds) kinetic phase with a slower kinetic phase. This implies that the back-reaction of the electron acceptor operating before incubation with $FeCl_3$ and Na_2S is replaced by a reaction with an electron carrier consisting of an iron-sulfur cluster. Because F_A and F_B are not present in this RC, vide infra, this carrier can be identified as the iron-sulfur cluster F_X. A comprehensive spectroscopic characterization of the acceptors responsible for both the 1.6-μs and 40-μs back-reactions with $P840^+$ are beyond the scope of this article and will be reported elsewhere (I. Vassiliev and J. Golbeck, work in progress).

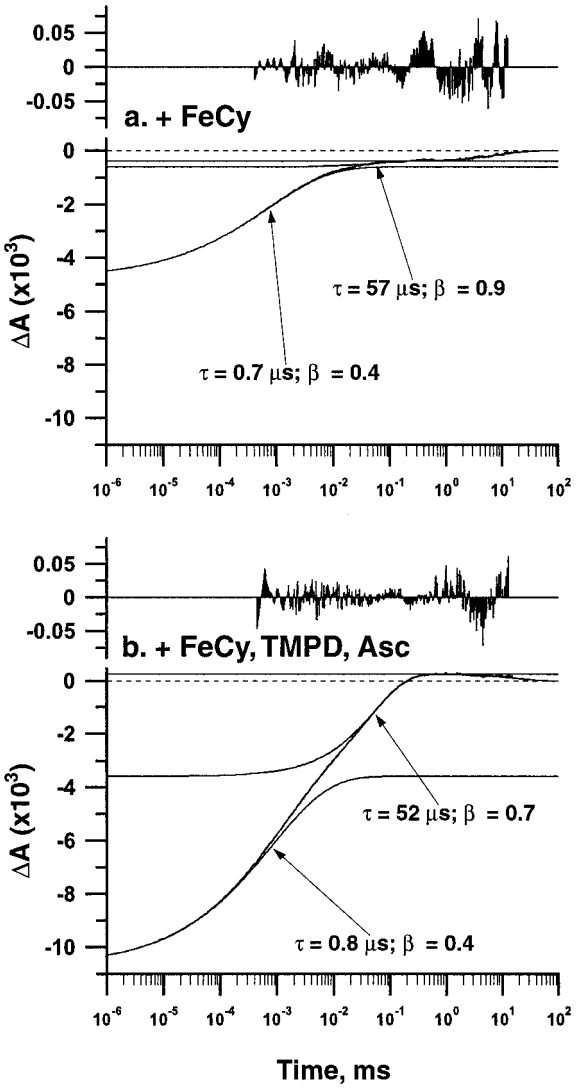

FIGURE 5 Effect of potassium ferricyanide (FeCy) on kinetics of absorbance changes at 835 nm in fraction 2 of RCCs isolated from *C. vibrioforme*. (*a*) RCC in 50 mM Tris buffer (pH 8), 0.05% β-DM, and 80 mM ferricyanide. (*b*) Same as *a* following addition of 50 μM TMPD and 10 mM sodium ascorbate. Bchl *a* concentration was 20 μM.

DISCUSSION

The primary goal of this work is to resolve the kinetics of photo-processes that contribute to NIR absorbance changes in the microsecond to millisecond time domain in RCs of green sulfur bacteria. For this purpose we devised an instrumental setup that allows kinetic measurements from 400 ns to 100 ms in the spectral range from 770 to 1025 nm. We have also developed a computer algorithm to analyze the kinetic data using the minimum number of components to obtain both a satisfactory quality of the fit in the whole spectral range and distinctive spectra for the amplitudes of the components. We show that in purified RCC complexes from *Chlorobium vibrioforme* there exist two different components in the microsecond to millisecond time domain that

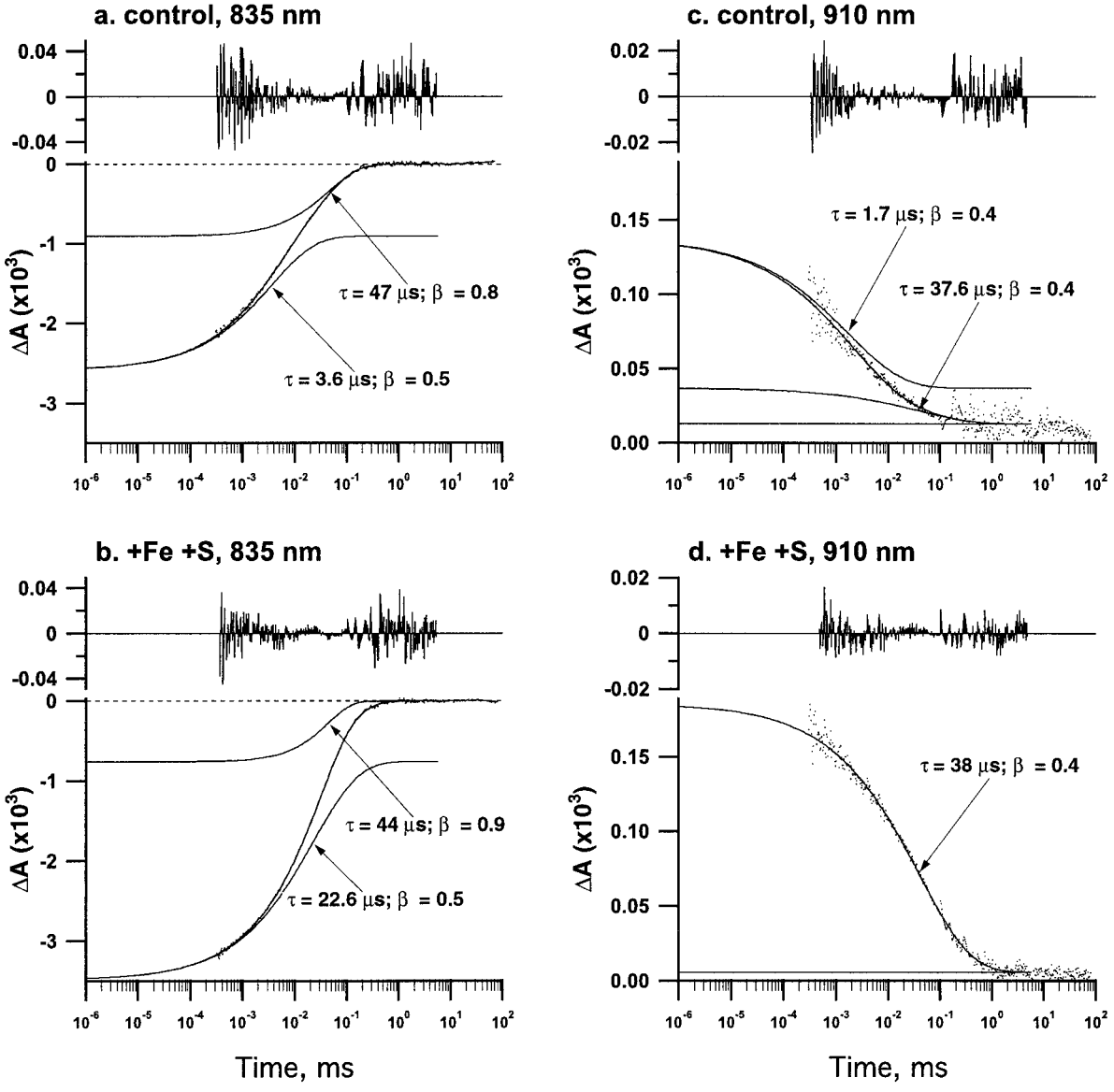

FIGURE 6 Effect of incubation of the isolated RCC (fraction 1) with sources of inorganic iron ($FeCl_3$) and sulfur (Na_2S) on the 835-nm (*a* and *b*) and 910-nm (*c* and *d*) kinetics of absorbance change. BChl *a* concentration was 5 μM. Other experimental conditions were as in Fig. 2. See Materials and Methods for details on iron-sulfur cluster reconstruction protocol.

have different but overlapping spectra. We find that kinetics of absorbance changes in the isolated RCC complex cannot be approximated by a simple monoexponential equation and that attempts to fit it using several exponentials lead to an arbitrarily large number of components. However, applying a stretched multi-exponential equation consistently leads to three components necessary to fit the kinetics in a wide time domain and over a wide range of wavelengths.

Even though the precision of parameters determined for the slowest component ($\tau \approx 10$ ms) is lower than for the faster components, its amplitude (1–2% relative to the sum of absolute amplitudes of the two fastest components at 830–840 nm) is consistently positive and does not show any significant wavelength dependence in the studied spectral range. At this point we cannot identify the origin of this component, but because a similar component is present in both the isolated membranes and the chlorosomes (unpublished observation), it is possible that it is related to some chlorosomal fragment still bound to the RCC complexes after purification.

The spectrum of the 40–100-μs component consists of a relatively broad bleaching with two minima at 810 and 825 nm and a broad positive band at wavelengths greater than 865 nm. The overall shape of the spectrum matches that reported earlier for the 67-μs decay of the ^{3}Bchl *a* of the FMO protein (Franken and Amesz, 1997) as well as that of

the differential photoinduced or chemically induced spectrum of the FMO protein (Miller et al., 1994). A correlation between the contribution of the 40–100-μs component and the FMO content in different RCC preparations (Figs. 1 and 2) serves as further support for the proposed assignment of this component. It is noteworthy that the FMO component (τ = 40–100 μs) has a relatively small deviation from pure exponential kinetics as indicated by the high stretch parameter (β = 0.7–1.0) necessary for its individual fitting at selected wavelengths as well as for global fitting in the whole spectral range.

The spectrum of the kinetic component with a lifetime of 1–1.6 μs has a sharp bleaching at 835 nm, a maximum at 805 nm, a broad positive band at wavelengths between 865 and 960 nm, and a broad negative band at wavelengths longer than 960 nm. The shape of this spectrum agrees in its overlapping domain with an earlier reported spectrum measured at 100 μs after flash in RC complexes of *Chlorobium tepidum* (Oh-Oka et al., 1998) as well as a spectrum of a 4-s component attributed to $P840^+$ reduction in RC complexes of *Prosthecochloris aestuarii* (Francke et al., 1997). It is also similar to the chemically-reduced-minus-oxidized difference spectrum of $P840^+$/P840, measured in the same sample (Fig. 3 *a*) and in a similar RC preparation from *Chlorobium vibrioforme* (Okkels et al., 1992).

The P840 component (τ = 1.6 μs) shows kinetics strongly deviating from pure exponential (β = 0.3–0.5), which implies that any measurement of this component in a relatively narrow time window and applying a pure exponential equation to fit the kinetics may lead to inconsistent values in its lifetime. Because the lifetime of this component is faster than the lifetimes reported for $P840^+$ reduction from cytochrome c_{551} (Albouy et al., 1997; Oh-Oka et al., 1997), it is most likely that in the RCC preparation used in this study the reduction of $P840^+$ occurs predominantly by a back-reaction with a bound electron acceptor preceding F_A and F_B. In agreement with this, the PscB protein carrying F_A and F_B was sub-stoichiometric in the samples used in the present study (see Fig. 1), and the EPR spectrum of F_A^-/F_B^- was barely detectable (not shown). On the one hand, the lifetime of the fast component is considerably slower than the lifetime of the back-reaction between A_0^- and $P840^+$ (20–35 ns) (Swarthoff et al., 1981). On the other hand, it is faster than the 50-μs component, which was removed by chaotrope treatment and then restored by addition of inorganic iron and sulfur and ascribed to F_X in a *Chlorobium vibrioforme* RC (Miller et al., 1992). It is also faster than the 700-μs component of $P840^+$ reduction observed in RCs from *Chlorobium tepidum* in which F_X was presumably present, but F_A and F_B were lost (Schmidt et al. 2000). Therefore, a possible candidate for $P840^+$ reductant in our RCC preparations could be an intermediate acceptor that operates between A_0 and F_X in PS I. The replacement of the 1.6-μs component with a slower phase (τ = 23 μs) upon incubation with $FeCl_3$ and Na_2S is consistent with the reconstruction of an iron-sulfur cluster, and this cluster now serves as the terminal electron acceptor in the RCC. Given the sub-stoichiometric amount of PscB in the RCC preparation, the reconstructed cluster is likely to be F_X. Two possibilities may be considered for the origin of the new tens-of-microseconds kinetic phase. First, this phase may be ascribed to forward electron donation from cytochrome c_{551} to P840 if this cytochrome is operational in the RCC and its reaction is faster than the back-reaction of F_X. Second, this phase may result from charge recombination between $P840^+$ and F_X^- in the case when the cytochrome c_{551} is either inactive or donates electrons to $P840^+$ slower than F_X^-. We were not able to measure absorbance changes in the 500–600-nm region attributable to cytochrome c_{551} using our previously described UV-Vis spectrophotometer (Shinkarev et al., 2000) either in the control RCC preparations or in the RCCs after treatment with $FeCl_3$ and Na_2S, which implies that this cytochrome is most likely inactive in our preparations. Therefore, reduction of $P840^+$ in the reconstructed samples apparently occurs due to direct charge recombination with F_X^-. Regardless of the nature of the partner in $P840^+$ reduction in the reconstructed RCCs, these results indicate that the initial RCC preparation possesses a terminal electron acceptor between A_0 and F_X.

Magnetic resonance data originally supported the existence of a functional quinone acceptor in *Chlorobium* RC (Kjær et al., 1998; Muhiuddin et al., 1999), although there is now a report to the contrary (van der Est et al., 1998). Optical kinetic studies (Kusumoto et al., 1999) failed to find its requisite spectroscopic signature on a biophysically meaningful time scale. Future studies of RC complexes of green sulfur bacteria, including an investigation of the back-reaction kinetics in the UV-Vis and their assignments to the electron carriers, will be necessary to resolve this controversy.

The deviation of the 1.6-μs component from monoexponential kinetics may be related to conformational heterogeneity in the *Chlorobium* RCC complexes and may indicate a distribution of electron transfer rates of $P840^+$ reduction. At wavelengths below 860 nm (where the S/N ratio is high) we could not obtain a multi-exponential fit that meets the residuals symmetry criterion with less than six exponentials (Fig. 2 *c*). This obviously does not make much biochemical sense, given that all derived components that are shorter than 70 μs in their lifetime appear to follow the same spectrum at different wavelengths (not shown). However, such a pattern may be considered as an indication of a rate distribution defined by a formula, $A(t) = \int_0^\infty F(\tau, 0)\exp(-t/\tau)d\tau$, where the amplitudes of different exponential components are placed on a grid of lifetimes. A robust solution for kinetics with distributed rate constant can be provided by a stretched exponential equation $A(t) = A_0\exp(-(t/\tau)^\beta)$, where the parameter β reflects the deviation from a purely exponential equation (for deri-

vation of this equation see Montrol and Bendler, 1984; Marshall, 1989).

Type II bacterial RCs have shown an increase in the broadness of the rate distribution of charge recombination coupled to protein relaxation at low temperatures where different conformation states can be said to be frozen in (Kleinfeld et al., 1984; McMahon et al., 1998). Similar effects were observed in the RCs of green filamentous bacteria (Becker et al., 1991). The description of electron transfer in type II bacterial RCs by the rate distribution equation was extensively derived by Bixon and Jortner presuming structural heterogeneity in the RCs resulting from continuous distribution of the energy gaps, reorganization energies, and electronic couplings (Bixon and Jortner 1986; Bixon et al., 1995). These fundamental mechanisms of electron-conformational interactions should extend to type I RCs, but the broadness of the rate distribution at a given temperature will depend on dynamic properties of a particular RC. A more detailed study of temperature dependencies of electron transfer reactions in *Chlorobium* RC will be necessary to link this observed non-exponential character of kinetics with existence of conformation substates. One way or another, the examples from type II bacterial reaction centers indicate that kinetics of electron transfer in a complex system like photosynthetic RCs should not be purely exponential in general due to the dynamic nature of the proteins. We proposed earlier that appearance of two exponential components in the kinetics of back-reactions of F_X, F_A, and F_B (Vassiliev et al., 1997; Shinkarev et al., 2000) may be a reflection of a process with a distributed rate constant. Recently we reanalyzed these data using a stretched-exponential model, and we were able to minimize the number of necessary components to just one stretched-exponential component for each of these acceptors (albeit with relatively high values of $\beta = 0.7–0.8$ in comparison with *Chlorobium* RCCs) (Vassiliev et al., 2001). The results of kinetic analyses, now in progress in our laboratory, indicate that there is a temperature-dependent distribution of rate constants in the back-reactions of A_1 and F_X in PS I. From a computational point of view, using a stretched-exponential equation is advantageous over a purely exponential one (given that the fit quality criteria are properly assessed), because even if a purely exponential decay takes place, the fit routine will simply yield a β value equal to 1.

Recently we isolated a RC complex of *Chlorobium tepidum* that retains a nearly stoichiometric P840/(F_A plus F_B) ratio as in the whole cells or isolated membranes as assayed by ratio of the intensities of EPR signals of $P840^+$ and F_A^-/F_B^- measured at 14 K (Vassiliev et al., 2000). We found that omission of the final purification steps, along with extra precautions to sustain anaerobiosis on all stages of the isolation procedure, results in a highly photoactive RC complex at the expense of purity. Preliminary analysis of the NIR kinetics of this intact RC complex shows a considerably higher contribution of the 70-μs component than found in the RC complex studied in the present work (unpublished observations). According to scanning transmission electron microscopic data, one FMO trimer interacts directly both with the periphery of the PscA homodimer and with a protruding knob that is likely to represent the PscB and PscD proteins. It is possible that a second FMO trimer is symmetrically bound from the other side of this knob, but that it can be easily dissociated from the complex cannot be excluded (Remigy et al., 1999). This explains both the variability of the FMO content per RC and the co-dissociation of FMO and PscB that leads to the loss of F_A and F_B even when the detergent treatment and purification of the RC complex are performed under strictly anaerobic conditions. Our densitometric estimates of 2.8 and 5.0 copies of monomeric FMO (i.e., ~1 and 2 trimers) per RC in the fractions 1 and 2, respectively, are in reasonable agreement with these structural data. These considerations agree with the earlier assumption that the FMO protein is integrated tightly with the RC, and a decrease of photochemical activity of the RC complex inevitably occurs following attempts to completely remove the FMO protein (Olson et al., 1976; Vasmel et al., 1983; Miller et al., 1994).

Almost all the spectra of the FMO protein and P840 were measured within the 770–900-nm spectral range. Absorbance changes at higher wavelengths, which are obviously more favorable due to lack of actinic effects on P840, have not been given adequate attention in previous studies. The photoreactions in isolated RC complexes of *Chlorobium tepidum* were studied by Kusumoto and co-workers by transient absorbance spectroscopy at 970 and 1150 nm, where positive absorbance changes were attributed to P840 oxidation (Kusumoto et al., 1999). However, no analysis of the whole spectral region that comprise these wavelengths was performed that might follow the spectral signatures of kinetic components, and these two wavelengths were selected from the spectrum (induced by steady-state illumination) published earlier for RC complexes isolated from *Chlorobium limicola* (Olson et al., 1976). Because the decay of ^{3}Bchl *a* of the FMO protein has a relatively long lifetime of 70 μs (at least comparable to that of forward donation from cytochrome c_{551}) it is quite possible that the absorbance changes due to FMO could have contributed to this spectrum. According to our results, the absorbance change of P840 goes negative at 970 nm, which is quite near to the crossover point at ~960 nm (Fig. 3 *a*).

CONCLUSIONS

Given the close spectral and kinetic overlap of the photoinduced absorbance changes of P840 and the FMO protein, approaches that utilize measurements at a single wavelength, which were quite successful in case of PS I and were thus far applied in a number of studies on *Chlorobium*, have an inherent limitation. Studies of *Chlorobium* RC complexes can benefit from global kinetic analysis at several

wavelengths, with supplementary information provided by alternative methods such as time-resolved and CW EPR spectroscopy.

The change of transient absorbance kinetics at both 835 nm and 910 nm following RC incubation with sources of inorganic iron and sulfur is consistent with a reconstruction of the F_X iron-sulfur cluster. Therefore, the 1.6-μs kinetics observed in the originally isolated complex may be attributed to an intermediate electron acceptor operating between A_0 and F_X.

We thank Hanne Linde Nielsen for technical assistance.

This work was supported by U.S. Department of Energy grant DE-FG-02–98-ER20314 to J.H.G. and I.R.V. and in part by the Danish National Research Foundation grant to H.V.S. and B.K.

REFERENCES

Albouy, D., J. N. Sturgis, U. Feiler, W. Nitschke, and B. Robert. 1997. Membrane-associated c-type cytochromes from the green sulfur bacterium *Chlorobium limicola* forma *thiosulfatophilum*: purification and characterization of cytochrome c(553). *Biochemistry.* 36:1927–1932.

Becker, M., V. Nagarajan, D. Middendorf, W. Parson, J. Martin, and R. Blankenship. 1991. Temperature dependence of the initial electron-transfer kinetics in photosynthetic reaction centers of *Chloroflexus aurantiacus. Biochim. Biophys. Acta.* 1057:299–312.

Bixon, M., and J. Jortner. 1986. Coupling of protein modes to electron-transfer in bacterial photosynthesis. *J. Phys. Chem.* 90:3795–3800.

Bixon, M., J. Jortner, and M. E. Michel-Beyerle. 1995. A kinetic-analysis of the primary charge separation in bacterial photosynthesis: energy gaps and static heterogeneity. *Chem. Phys.* 197:389–404.

Feiler, U., and G. Hauska. 1996. The reaction center from green sulfur bacteria. *In* Anoxygenic Photosynthetic Bacteria. Kluwer Academic Publishers, Dordrecht, The Netherlands. 665–685.

Fling, S. P., and D. S. Gregerson. 1986. Peptide and protein molecular-weight determination by electrophoresis using a high-molarity Tris buffer system without urea. *Anal. Biochem.* 155:83–88.

Fowler, C. F., N. A. Nugent, and R. C. Fuller. 1971. The isolation and characterization of a photochemically active complex from *Chloropseudomonas ethylica. Proc. Natl. Acad. Sci. U.S.A.* 68:2278–2282.

Franken, E. M., and J. Amesz. 1997. Electron transport and triplet formation in membrane fragments of the green sulfur bacterium *Prosthecochloris aestuarii. Biochim. Biophys. Acta.* 1319:214–222.

Francke, C., H. P. Permentier, E. M. Franken, S. Neerken, and J. Amesz. 1997. Isolation and properties of photochemically active reaction center complexes from the green sulfur bacterium *Prosthecochloris aestuarii. Biochemistry.* 36:14167–14172.

Golbeck, J. H. 1994. Photosystem I in cyanobacteria. *In* The Molecular Biology of Cyanobacteria. D. A. Bryant, editor. Kluwer Academic Publishers, Dordrecht, The Netherlands. 179–220.

Hager-Braun, C., U. Jarosch, G. Hauska, W. Nitschke, and A. Riedel. 1997. EPR studies of the terminal electron acceptors of the green sulfur bacterial reaction centre: revisited. *Photosynth. Res.* 51:127–136.

Kjær, B., N. U. Frigaard, F. Yang, B. Zybailov, M. Miller, J. H. Golbeck, and H. V. Scheller. 1998. Menaquinone-7 in the reaction center complex of the green sulfur bacterium *Chlorobium vibrioforme* functions as the electron acceptor A_1. *Biochemistry.* 37:3237–3242.

Kjær, B., Y. S. Jung, L. A. Yu, J. H. Golbeck, and H. V. Scheller. 1994. Iron-sulfur centers in the photosynthetic reaction center complex from *Chlorobium vibrioforme*: differences from and similarities to the iron-sulfur centers in photosystem I. *Photosynth. Res.* 41:105–114.

Kleinfeld, D., M. Y. Okamura, and G. Feher. 1984. Electron-transfer kinetics in photosynthetic reaction centers cooled to cryogenic temperatures in the charge-separated state: evidence for light-induced structural changes. *Biochemistry.* 23:5780–5786.

Kramer, H., T. J. Aartsma, and J. Amesz. 1996. Excited states and charge separation in membranes of the green sulfur bacterium *Prosthecochloris aestuarii. Photochem. Photobiol.* 64:26–31.

Kusumoto, N., P. Sétif, K. Brettel, D. Seo, and H. Sakurai. 1999. Electron transfer kinetics in purified reaction centers from the green sulfur bacterium *Chlorobium tepidum* studied by multiple-flash excitation. *Biochemistry.* 38:12124–12137.

Marshall, D. B. 1989. Statistical considerations in the analysis of dispersive kinetics data as discrete or continuous distributions of rate constants. *Anal. Chem.* 61:660–665.

McMahon, B. H., J. D. Muller, C. A. Wraight, and G. U. Nienhaus. 1998. Electron transfer and protein dynamics in the photosynthetic reaction center. *Biophys. J.* 74:2567–2587.

Miller, M., R. P. Cox, and J. M. Olson. 1994. Low-temperature spectroscopy of isolated FMO-protein and a membrane-free reaction-center complex from the green sulfur bacterium *Chlorobium tepidum. Photosynth. Res.* 41:97–103.

Miller, M., X. Liu, S. Snyder, M. Thurnauer, and J. Biggins. 1992. Photosynthetic electron-transfer reactions in the green sulfur bacterium *Chlorobium vibrioforme:* evidence for the functional involvement of iron-sulfur redox centers on the acceptor side of the reaction center. *Biochemistry.* 31:4354–4363.

Montrol, E. W., and J. T. Bendler. 1984. On Levy (or Stable) distributions and the Williams-Watts model of dielectric relaxation. *J. Stat. Phys.* 34:129–162.

Muhiuddin, I. P., S. E. J. Rigby, M. C. W. Evans, J. Amesz, and P. Heathcote. 1999. ENDOR and special TRIPLE resonance spectroscopy of photoaccumulated semiquinone electron acceptors in the reaction centers of green sulfur bacteria and heliobacteria. *Biochemistry.* 38:7159–7167.

Neerken, S., H. P. Permentier, C. Francke, T. J. Aartsma, and J. Amesz. 1998. Excited states and trapping in reaction center complexes of the green sulfur bacterium *Prosthecochloris aestuarii. Biochemistry.* 37:10792–10797.

Oh-Oka, H., M. Iwaki, and S. Itoh. 1997. Viscosity dependence of the electron transfer rate from bound cytochrome c to P840 in the photosynthetic reaction center of the green sulfur bacterium *Chlorobium tepidum. Biochemistry.* 36:9267–9272.

Oh-Oka, H., S. Kakutani, S. Kamei, H. Matsubara, M. Iwaki, and S. Itoh. 1995a. Highly purified photosynthetic reaction center (PscA/cytochrome $c_{551})_2$ complex of the green sulfur bacterium *Chlorobium limicola. Biochemistry.* 34:13091–13097.

Oh-Oka, H., S. Kamei, H. Matsubara, M. Iwaki, and S. Itoh. 1995b. Two molecules of cytochrome c function as the electron donors to P840 in the reaction center complex isolated from a green sulfur bacterium *Chlorobium tepidum. FEBS Lett.* 365:30–34.

Oh-Oka, H., S. Kamei, H. Matsubara, S. Lin, P. I. van Noort, and R. E. Blankenship. 1998. Transient absorption spectroscopy of energy-transfer and trapping processes in the reaction center complex of *Chlorobium tepidum. J. Phys. Chem. B.* 102:8190–8195.

Okkels, J. S., B. Kjær, O. Hansson, I. Svendsen, B. L. Moller, and H. V. Scheller. 1992. A membrane-bound monoheme cytochrome-c551 of a novel type is the immediate electron donor to P840 of the *Chlorobium vibrioforme* photosynthetic reaction center complex. *J. Biol. Chem.* 267:21139–21145.

Olson, J. M. 1998. Chlorophyll organization and function in green photosynthetic bacteria. *Photochem. Photobiol.* 67:61–75.

Olson, J. M., K. D. Philipson, and K. Sauer. 1973. Circular dichroism and absorption spectra of bacteriochlorophyll-protein and reaction center complexes from *Chlorobium thiosulfatophilum. Biochim. Biophys. Acta.* 292:206–217.

Olson, J. M., R. C. Prince, and D. C. Brune. 1976. Reaction-center complexes from green bacteria. *Brookhaven Symp. Biol.* 13:238–246.

Parrett, K. G., T. Mehari, and J. H. Golbeck. 1990. Resolution and reconstitution of the cyanobacterial photosystem I complex. *Biochim. Biophys. Acta.* 1015:341–352.

Remigy, H. W., H. Stahlberg, D. Fotiadis, S. A. Muller, B. Wolpensinger, A. Engel, G. Hauska, and G. Tsiotis. 1999. The reaction center complex from the green sulfur bacterium *Chlorobium tepidum*: a structural analysis by scanning transmission electron microscopy. *J. Mol. Biol.* 290: 851–858.

Schmidt, K. A., S. Neerken, H. P. Permentier, C. Hager-Braun, and J. Amesz. 2000. Electron transfer in reaction center core complexes from the green sulfur bacteria *Prosthecochloris aestuarii* and *Chlorobium tepidum. Biochemistry.* 39:7212–7220.

Schmidt, K. A., and H. W. Trissl. 1998. Combined fluorescence and photovoltage studies on chlorosome containing bacteria. II. Whole cells and chlorosome-depleted membranes of *Chlorobium limicola. Photosynth. Res.* 58:57–70.

Scott, M. P., B. Kjær, H. V. Scheller, and J. H. Golbeck. 1997. Redox titration of two [4Fe-4S] clusters in the photosynthetic reaction center from the anaerobic green sulfur bacterium *Chlorobium vibrioforme. Eur. J. Biochem.* 244:454–461.

Shinkarev, V. P., I. R. Vassiliev, and J. H. Golbeck. 2000. A kinetic assessment of the sequence of electron transfer from F_X to F_A and further to F_B in photosystem I: the value of the equilibrium constant between F_X and F_A. *Biophys. J.* 78:363–372.

Swarthoff, T., P. Gast, A. J. Hoff, and J. Amesz. 1981. Photooxidation and triplet formation of the primary electron donor of the green photosynthetic bacterium *Prosthecochloris aestarii*, observed with EPR spectroscopy. *FEBS Lett.* 130:93–98.

Sybesma, C., and W. J. Vredenberg. 1963. Evidence for a reaction center P840 in the green photosynthetic bacterium *Chloropseudomonas ethylicum. Biochim. Biophys. Acta.* 75:439–441.

Van de Meent, E., M. Kobayashi, C. Erkelens, P. Van Veelen, S. Otte, K. Inoue, T. Watanabe, and J. Amesz. 1992. The nature of the primary electron acceptor in green sulfur bacteria. *Biochim. Biophys. Acta.* 1102:371–378.

van der Est, A., C. Hager-Braun, W. Leibl, G. Hauska, and D. Stehlik. 1998. Transient electron paramagnetic resonance spectroscopy on green-sulfur bacteria and heliobacteria at two microwave frequencies. *Biochim. Biophys. Acta.* 1409:87–98.

Vasmel, H., T. Swarthoff, H. J. M. Kramer, and J. Amesz. 1983. Isolation and properties of a pigment-protein complex associated with the reaction center of the green photosynthetic sulfur bacterium *Prosthecochloris aestuarii. Biochim. Biophys. Acta.* 725:361–367.

Vassiliev, I. R., M. L. Antonkine, and J. H. Golbeck. 2001. Iron-sulfur clusters in type I reaction centers. *Biochim. Biophys. Acta.* In press.

Vassiliev, I. R., Y. S. Jung, M. D. Mamedov, A. Y. Semenov, and J. H. Golbeck. 1997. Near-IR absorbance changes and electrogenic reactions in the microsecond-to-second time domain in photosystem I. *Biophys. J.* 72:301–315.

Vassiliev, I. R., M. T. Ronan, G. Hauska, and J. H. Golbeck. 2000. The bound electron acceptors in green sulfur bacteria: resolution of the g-tensor for the FX iron-sulfur cluster in *Chlorobium tepidum*. *Biophys. J.* 78:3160–3169.

Zhou, W. L., R. LoBrutto, S. Lin, and R. E. Blankenship. 1994. Redox effects on the bacteriochlorophyll *a*-containing Fenna-Matthews-Olson protein from *Chlorobium tepidum. Photosynth. Res.* 41:89–96.